Journal of Photochemistry and Photobiology A: Chemistry 216 (2010) 35–43

Contents lists available at ScienceDirect

Journal of Photochemistry and Photobiology A: Chemistry

journal homepage: www.elsevier.com/locate/jphotochem

# Dye sensitized membranes within mesoporous $TiO_2$: Photocurrents in aqueous solution

Dereje Hailu Taffa[a,1], Murugavel Kathiresan[a,1], Tamara Arnold[a,1], Lorenz Walder[a,*,1], Martin Erbacher[b], Daniela Bauer[b], Franz-Peter Montforts[b], Jörg Nordmann[a,2], Markus Haase[a,2]

[a] Institute of Chemistry, University of Osnabrück, Barbarastrasse 7, D-49069 Osnabrück, Germany
[b] Institute of Organic Chemistry, University of Bremen, Leobenerstrasse NW 2C, D-28359 Bremen, Germany

ARTICLE INFO

*Article history:*
Received 2 June 2010
Received in revised form 27 August 2010
Accepted 1 September 2010
Available online 21 September 2010

*Key words:*
DSSCs
Mesoporous $TiO_2$
Membrane
Porphyrin
Photocurrent

ABSTRACT

Mesoporous $TiO_2$ film electrodes were modified with membranes consisting of alkyl phosphonic acids with either a sulphonate or pyridinium head group. Dyes (substituted porphyrins (**1**, **2**, and **3**), a substituted chlorin (**4**) and a substituted Ru tris-bipyridyl complex (**5**)) with tailored ionic (carboxylates, sulfonates, and ammonium) and hydrophobic functionalities were synthesized. The membrane modified electrodes were loaded with these dyes by self-assembling based on mutual charge compensation and hydrophobic interactions. The membrane electrodes can generate photocurrents upon white light illumination (16.5 mW/cm$^2$) in the range of 20–50 μA/cm$^2$ in aqueous 0.1 M KI solution. Dyes **3** and **4** perform better on the pyridinium membrane than directly attached via their carboxylate functionality. This demonstrates charge injection through the membrane into the conduction band of $TiO_2$. ZINDO/S calculations indicate that the pyridinium head group assists this process.



## 1. Introduction

Dye sensitized solar cells (DSSCs) are the subject of intensive research as an alternative to conventional silicon solar cells [1]. DSSCs based on nano-crystalline $TiO_2$ sensitized with polypyridyl ruthenium complexes achieve a sun-light to electric-power conversion efficiency of nearly 11% using organic solvents and the $I^-/I_3^-$ couple as a mediator [2]. The presence of water in the organic solvent can break the sensitizer $TiO_2$ coordinative bond, a drawback which is partially circumvented by the use of amphiphilic dyes and co-adsorbents [3]. Such surface modification is also beneficial with respect to suppression of the back electron transfer from the CB of $TiO_2$ to the triiodide thereby increasing $V_{oc}$ [4]. In line with these observations, pure water or water–alcohol mixture based solvents yield only low power conversion efficiencies in the range of 0.5–2% for different ruthenium dyes [5], natural dyes extracted from plants [6], or Au nano-particles on $TiO_2$ [7].

On the other hand, the natural photosynthetic system is water based – or more accurately – based on a bilayer membrane in water and relies on a photo-induced vectorial electron transfer through that membrane [8]. A cascade of redox centers with appropriately tuned reduction potential and suitable location guides the electron through the membrane to the terminal acceptor. Obviously such architecture reduces the probability for back electron transfer for the sake of some loss in reduction potential. The idea of using a membrane has so far not been exploited for dye sensitized nano-crystalline $TiO_2$ photoelectrodes. The direct injection of the electron from the excited sensitizer into the conduction band of $TiO_2$ is thought to proceed fast and with high quantum yield only, if the sensitizer is directly grafted onto the semiconductor surface and if a surface dipole assists the directionality of this process [9].

Recently we reported on the post functionalization of mesoporous $TiO_2$ with alkyl phosphonic acids bearing a charged head group. The self-assembling process leads to a relatively disordered membrane on the inner walls of the $TiO_2$ channels. The membrane can further be loaded with different electroactive guest molecules based on a combination of hydrophobic and electrostatic interactions [10]. In this communication we have extended the same principle to prepare a photoanode for DSSC application. It is shown that different positively or negatively charged dye molecules with additional hydrophobic substituents can be efficiently bound in a supramolecular fashion on a membrane-covered nano-crystalline $TiO_2$ electrode, and that electron injection through the membrane into $TiO_2$ is still possible. Furthermore, experimental and theoretical evidence is presented, that electroactive head groups with well adjusted reduction potential (such as pyridinium) can assist the vectorial electron transfer. Probably this involves an electron hoping mechanism from pyridinium to pyridinium and helps to guide

* Corresponding author. Tel.: +41 541 9692495.
*E-mail address:* LoWalder@uos.de (L. Walder).
[1] OCII.
[2] ACI.

1010-6030/$ – see front matter © 2010 Elsevier B.V. All rights reserved.
doi:10.1016/j.jphotochem.2010.09.003

the electron along the membrane surface and to inject it into the conduction band (CB) of the underlying $TiO_2$.

Using alkylphosphonates with positively or negatively charged head groups, it is possible to load the membrane with many available dyes without necessitating the synthetically tedious introduction of a $TiO_2$ anchoring group on the dye. Thus, the new technique consisting of sequential self-assembling processes shows high flexibility with a limited set of building blocks. It allows realizing new supramolecular functions based on an unprecedented architectural complexity achievable within the mesopores of $TiO_2$.

The efficiencies presented are much lower than for N3 sensitized mesoporous $TiO_2$ in organic solvent/electrolyte and even in water (without a membrane) the N3 modification shows higher currents. The aim of the study is a "proof of principle" concerning a new type of surface modification; parameter optimization is not the focus.

## 2. Experimental

### 2.1. Reagents

4,4′-Dinonyl-2,2′-dipyridyl (Aldrich), Ru 535 dye (Solaronix), and cis-dichloro(2,2′-bipyridine)ruthenium (II) dihydrate, 99% (ABCR) were used as received. All starting materials for the synthesis of porphyrins were from Fluka, Merck or Sigma–Aldrich and used without further purification. All solvents were purified and dried by standard methods.

### 2.2. Synthesis

The intermediates (**1′** and **3′**, Scheme 1) for the synthesis of the porphyrin **1** and **3** were synthesized according to reported procedures [11]. The chlorine, 3,3′-[(cis-7RS,8SR)-7-(Dimethylcarbamoylmethyl)-8-heptyl-2,7,12,18-tetramethyl-7,8-dihydro-21H,23H-porphyrin-13,17-diyl]-dipropionic acid (**4**) was synthesized following a procedure reported earlier [12].

#### 2.2.1. [13,17-Bis (2′(propanoylamino)-ethanesulfonic acid)-2,7,12,18-tetramethyl-porphyrinato]-zinc(II) (*1*)

To a solution of [13,17-bis(propionic acid)-2,7,12,18-tetramethylporphyrinato]-zinc(II) **1′** (30 mg, 59 μmol) and triethylamine (22 μl, 130 μmol) in THF (50 ml) were added 22 μl (236 μmol) ethyl chloroformate was added at −15 °C. After 15 min a solution of taurine (2-aminoethanesulfonic acid, 44.3 mg, 354 μmol) and triethylamine (50 μl, 354 μmol) in water/THF (v:v 1:1) was added and the mixture was stirred for additional 30 min under ambient temperature. The solvent and the volatile compounds were removed in a rotary evaporator and the residue was first gel-filtered (sephadex LH-20, methanol/water (v:v 4:1) and afterwards purified by reversed phase column chromatography (RP-18 silica gel, methanol/water 4 + 1). Crystallization from methanol/diethylether yielded the product (**1**) as a dark red solid (33.9 mg, 73%).

1H NMR (200 MHz, d6-DMSO): $\delta$ = 2.46 (m, 4H), 3.04 (m, 4H), 3.29 (m, 4H), 3.58, 3.62, 3.70, 3.73 (4s, 12H), 4.31 (m, 4H), 7.94 (m, 2H), 9.18, 9.19 (2s, 2H), 10.06, 10.08, 10.13, 10.17 (4s, 4H).

ESI-MS: $[M+Na]^+$: *m/z* 809.3, $[M-H]^-$: *m/z* 785.1.

#### 2.2.2. 13, 17-Bis [3′-(propanoylamino)-bromopropyl]-2,7,12,18-tetramethylporphyrin (*2′*)

[13,17-bis(propionic acid)-2,7,12,18-tetramethylporphyrinato]-zinc(II) **1′** (73 mg, 0.13 mmol), 3-bromo-1-aminopropane hydrobromide (111 mg, 0.5 mmol), (benzotriazol-1-yloxy)tris (dimethylamino)phosphonium hexafluorophosphate (BOP, 225 mg, 0.5 mmol) and triethylamine (0.1 ml, 0.7 mmol) were dissolved in dry THF (10 ml) and stirred for 18 h under an argon atmosphere at room temperature. The solution was given to brine (40 ml) and extracted with dichloromethane. The organic phase was washed with 2N aq. HCl, water, sat. $NaHCO_3$ solution, water and filtered through cotton. After evaporation, flash chromatography (silica gel, dichloromethane/methanol 9 + 1) and additional column chromatography (silica gel, dichloromethane/ethanol 25 + 1) yielded 92 mg (122 μmol, 94%) of **2′** as a purple solid.

$^1$H NMR (200 MHz, $CDCl_3$ + 10 μl d5-pyridine): $\delta$ = −3.90 (2 s, 2H), 1.53 (m, 4H), 2.80 (m, 4H), 3.05–3.17 (m, 8H), 3.57, 3.59, 3.72, 3.74 (4s, 12H), 9.08, 9.09 (2s, 2H), 9.99, 10.06, 10.09, 10.22 (4s, 4H).

ESI-MS: $[M+H]^+$: *m/z* 749.2, $[M+Cl]^-$: *m/z* 783.1.

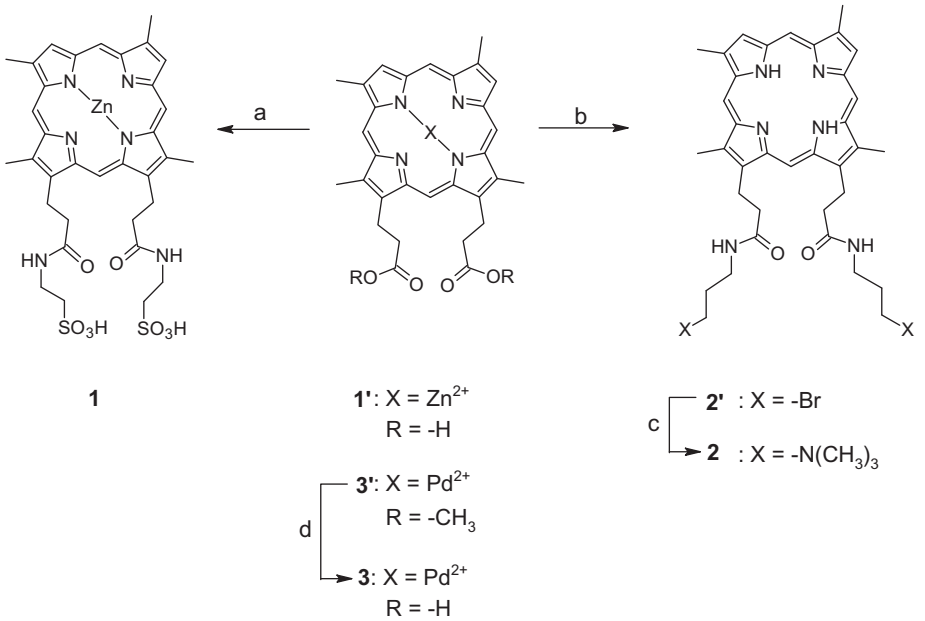


**Scheme 1.** (1) Ethyl chloroformate, triethylamine, THF, −15 °C, 15 min; (2) taurine, triethylamine, rt, 30 min. (a) 3-Bromo-1-aminopropane hydrobromide, BOP, THF, rt, 18 h. (b) 33% trimethylamine in ethanol/THF, 50 °C, 18 h. (c) 5N aq. KOH, THF, 24 h, reflux.

*2.2.3. 13, 17-Bis [N,N,N-3′-(propanoylamino)-propan-1-trimethyl ammonium bromide]-2,7,12,18-tetramethylporphyrin (**2**)*

13,17-Bis[3′-(propanoylamino)-bromopropyl]-2,7,12,18-tetramethylporphyrin **2**′ (20 mg, 26.6 μmol) was dissolved in methanol (15 ml). After adding a 33% solution of trimethylamine in ethanol (15 ml) the mixture was stirred for 18 h at 50 °C. Removal of the solvent and volatile compounds in a rotary evaporator and recrystallisation from methanol/diethylether yielded 15.8 mg (**4**) (18.2 μmol, 91%) of **2**.

$^1$H NMR (200 MHz, d6-DMSO): $\delta = -4.1$ (s, 2H), 1.25 (m, 4H), 2.21 (s, 18H), 2.61 (m, 4H), 2.91 (m, 4H), 3.09 (m, 4H), 3.64, 3.69, 3.74, 3.78 (4s, 12H), 4.40 (m, 4H), 8.07 (m, 2H), 9.36, 9.38 (2s, 2H), 10.33, 10.37 (2s, 4H).

ESI-MS: $[M-2Br]^{2+}$: $m/z$ 354.2, $[M-Br]^-$: $m/z$ 787.4.

*2.2.4. [13,17-Bis (propionic acid)-2,7,12,18-tetramethylporphyrinato]-palladium(II) (**3**)*

[13,17-Bis(propionic acid dimethylester)-2,7,12,18-tetramethylporphyrinato]-palladium (II) 3′ (200 mg, 0.31 mmol) was dissolved in THF (20 ml). After addition of 5N aq. KOH (20 ml), the reaction mixture was stirred under argon atmosphere for 18 h at 70 °C. The colourless THF phase was discarded and 5N aq. HCl (25 ml) and tert-butyl methyl ether (20 ml) were carefully added to the aqueous phase, which led to the separation of a precipitate at the phase boundary. The suspension was filtered through a Buchner funnel. Drying of the collected solid in high vacuum yielded palladium (II) deuterioporphyrin (3) 185 mg (0.30 mmol, 97%) as a deep red compound.

$^1$H NMR (200 MHz, d6-DMSO): $\delta = 2.82$ (m, 4H), 3.57, 3.62, 3.68, 3.72 (4s, 12H), 4.30 (m, 4H), 9.25, 9.27 (2s, 2H), 10.31, 10.32, 10.35, 10.36 (4s, 4H).

ESI-MS: $[M-H]^-$: $m/z$ 611.1.

*2.2.5. Bis(2,2′-bipyridyl)(4,4′-dinonyl-2,2′-bipyridyl)ruthenium(II) dichloride (**5**)*

4,4′-Dinonyl-2,2′-dipyridyl (316 mg, 0.77 mmol) and cis-dichloro(2,2′-bipyridine)ruthenium (II) dihydrate (300 mg, 0.62 mmol) were refluxed in 5:1 methanol:acetic acid (15 ml) under argon. After the mixture turned translucent orange (6 h), the reaction was cooled and evaporated in vacuo to yield the crude product, which was dissolved in 5 ml acetonitrile, slowly dropped into 100 ml anhydrous diethyl ether, and the precipitate was filtered. The residue were dissolved in a minimum amount of distilled water (4 ml) and gently drawn through the filter by suction to remove water-insoluble components. The filtrate containing the complex was evaporated under reduced pressure and dried to yield a dark translucent orange complex **5** (500 mg, 87%).

$^1$H NMR (250 MHz, CD3OD, $\delta$) 8.73 (d, 4H), 8.65 (s, 2H), 8.15 (t, 4H), 7.84 (d, 4H), 7.53 (d, 2H), 7.51 (m, 4H), 7.38 (d, 2H), 2.87 (t, 4H), 1.76 (bs, 4H), 1.35 (bs, 24H), 0.89 (t, 6H).

*2.3. Preparation of the dye sensitized $TiO_2$ electrodes*

Mesoporous $TiO_2$ thin films were prepared on conducting F-doped tin oxide (FTO) (2.2 mm, 15 Ω cm$^{-2}$, LOF) glass using a commercially available $TiO_2$ paste (particle size 14.5–21.6 nm, surface area 103 m$^2$ g$^{-1}$ (NTERA, Dublin, Ireland), and fired at 450 °C as reported earlier to yield a $TiO_2$ layer with a roughness factor in the range of 100–140 (cm$^{-2}$ μm$^{-1}$) [10a]. Notably, the resulting $TiO_2$ mesoporous material is optimized for electrochromic properties (large specific area, little or no haze, good electronic conductivity) rather than DSSC applications. Films prepared in this manner were transparent and have an average thickness of 3–4 μm (Supporting Information, Fig. 5).

The functionalization of the mesoporous $TiO_2$ thin films (1 cm$^2$) with the membrane was performed by immersing the $TiO_2$ plates in 1 mM methanolic solution of the phosphonic acids overnight. They were then carefully washed with the same solvent and air dried. The resulting membrane functionalized $TiO_2$ electrodes are designated as $TiO_2$/Pho-$C_{14}$-$Py^+$ and $TiO_2$/Pho-$C_{14}$-$SO_3^-$, respectively. The modification of the films was monitored by FT-IR spectroscopy (VERTEX-70, BRUKER) [10a]. The as prepared films were dipped in to a 0.5 mM stirred dye solution in methanol (**1**–**4**) or water (**5**) for 15 min. Finally, the electrodes were rinsed with the respective solvents. For comparison electrodes with Ru 535 (N3) dye directly coordinated to $TiO_2$ were prepared as reported [13].

UV–vis absorption spectra with dyes in solution (in Methanol: THF (**1**–**4**) or water (**5**)) or on a $TiO_2$/membrane electrode were measured using a photodiode array Agilent 8453 UV–visible spectrophotometer (Hewlett Packard). Surface concentration ($\Gamma$) on $TiO_2$ or on membrane modified $TiO_2$ (Table 1) were calculated from UV–vis spectra using the longer wave length Q bands and corrected for the roughness (ca.400). Emission spectra were measured in methanol (**1**–**4**) and water (**5**) with a spectrofluorometer, Fluorolog 3 (SPEX); the data were used to calculate excited state potentials of the dyes.

*2.4. Photoelectrochemical measurements*

A 450 W xenon light source (Oriel, USA) was used in combination with two filters GG 435 (Schott Glas) and BG 38 (Präzisions Glas and Optik GmbH, Germany) limiting the white light in the vis. range 420–800 nm with an intensity of 16.5 mW/cm$^2$. For monochromatic light illuminations a Metrospec (AMKO) monochromator was used in line with the cut-off filters. The light intensity reaching the electrode surface was measured with a calibrated AvaSpec-3648 spectrometer (Avantes, USA) equipped with a sine collector. The spectrometer was calibrated with a calibrated light source Avalight-HAL-CAL (Avantes, USA) yielding intensity errors <5%. The photocurrent was measured in a three electrode arrangement with a homemade photoelectrochemical cell fitted with quartz cuvette of path length 10 mm. The dye sensitized $TiO_2$ served as working electrode (illuminated area 0.5 cm$^2$), a platinum wire as counter and an Ag/AgCl (3MKCl) system as reference electrode. Aqueous solutions of 0.1 M KI were used as electrolyte. The potential of the working electrode was controlled by an Autolab Potentiostat PGSTAT 20 interfaced with a personal computer running under GPES for Windows, version 4.9 (ECO Chemie, Netherlands).

The incident photon to current conversion efficiency (IPCE) value at a given wave length was calculated following Eq. (1),

$$\mathrm{IPCE}(\lambda) = \frac{1240 \times I_{sc}}{\lambda \Phi} \quad (1)$$

where λ is the wave length (nm), $I_{sc}$ the short circuit photocurrent density (μA/cm$^2$) and $\Phi$ is the incident power flux (μW/cm$^2$).

Absorbed photon to current efficiency (APCE) determines the portion of absorbed photons that generate electrons in the external circuit. The relation between IPCE and APCE is shown in Eq. (2), where LHE corresponds to the light harvesting efficiency. LHE quantifies absorbance of monochromatic light by a device as a function of absorption and it is given by Eq. (3).

$$\mathrm{APCE}(\lambda) = \frac{\mathrm{IPCE}(\lambda)}{\mathrm{LHE}(\lambda)} \quad (2)$$

$$\mathrm{LHE}(\lambda) = 1 - 10^{-\mathrm{abs}(\lambda)} \quad (3)$$

## 3. Results and discussion

Mesoporous $TiO_2$ film electrodes (ca. 3 μm thick) were prepared by doctor blade technique (see Section 2) on FTO coated

**Table 1**
Absorption and emission data for the different dyes in solution, on membranes directly attached to $TiO_2$.

| Dye | $\varepsilon$ ($10^3$ $M^{-1}$ $cm^{-1}$) ($\lambda_{max}$) | $\lambda_{em}$ | $\lambda_{max}$ ($TiO_2$) | $\lambda_{max}$ ($TiO_2$-membrane) | $\Gamma$ (mol $cm^{-2}$) × $10^{10}$ |
|---|---|---|---|---|---|
| **1** | 69 (405), 7.4 (538), 6.5 (572) | 577, 630 | – | 542, 576 | 1.5 |
| **2** | 168 (395), 16.8 (495), 7.1 (526), 21.7 (565) | 619, 685 | – | 498, 529,568 | 0.42 |
| **3** | 139 (391), 16.2 (510), 39.7 (543) | 547, 623, 690 | 517, 548 | 513, 545 | 0.62 (1.2) |
| **4** | 167.5 (391), 13.4 (488), 52.1 (645) | – | 496, 646 | 496, 644 | 0.4 (1.1) |
| **5** | 45 (287), 13.8 (460) | 635 | – | 461 | 1.5 |

Absorption data were obtained in water (**5**), methanol: THF (1:1) (**1**–**4**).
Values in brackets are for dyes directly coordinated to $TiO_2$.
$\lambda_{em}$: emission wavelengths were obtained from fluorescence spectroscopy, excitation wave lengths are 382, 364, 401, and 455 for dyes **1**–**3** and **5**, respectively.

glass. They were then modified with one of the phosphonated alkanes with charged head group (Pho-$C_{14}$-$Py^+$, Pho-$C_6$-$Vio^{2+}$ or Pho-$C_{14}$-$SO_3^-$) to yield the corresponding membrane covered $TiO_2$ electrodes $TiO_2$/Pho-$C_{14}$-$Py^+$, $TiO_2$/Pho-$C_6$-$Vio^{2+}$ or $TiO_2$/Pho-$C_{14}$-$SO_3^-$, respectively, by self-assembling from 1 mM methanolic solutions, as presented in Fig. 1 and as reported earlier [10]. The outer part of the membrane coated $TiO_2$ electrodes was further modified by the porphyrin (**1**–**3**), chlorine (**4**) and polypyridyl Ruthenium(II) (**5**) again using self-assembling techniques from the appropriate solvent system (see Fig. 1 and exp. part for their structure). The dyes **1**–**5** were prepared on purpose to bind by combined electrostatic and hydrophobic interaction to the outer membrane plane. Thus dyes **1**, **4** and **3** with negative charge in their periphery are tailored for binding to $TiO_2$/Pho-$C_{14}$-$Py^+$, $TiO_2$/Pho-$C_6$-$Vio^{2+}$ and dyes **2** and **5** for $TiO_2$/Pho-$C_{14}$-$SO_3^-$, respectively (arrows in Fig. 1). The potential of further hydrophobic interaction is build into the dyes **4** and **5** and relies on alkyl chain intercalation (gray region in Fig. 1). Notably, dyes **3** and **4** with their carboxylic acid functionalities in the periphery can be attached in two ways to $TiO_2$, (i) using $TiO_2$/Pho-$C_{14}$-$Py^+$ and based on the new electrostatic/hydrophobic interactions, or (ii) by direct coordination of –COOH to $TiO_2$. Principally, the porphyrins (**1**–**3**) and chlorine (**4**) cores are not suited for high efficiency white light energy conversion (narrow absorption band). They were chosen because the introduction of charges and alkyl chains is synthetically feasible, allowing us to check the membrane approach.

In solution the porphyrin macrocyclic dyes and the chlorin (**4**) exhibit an intense absorption band at about 400 nm (the Soret band), followed by weaker absorptions (Q bands) at higher wavelengths (from 450 to 700 nm). The Soret band is quite similar in all four spectra with a peak maximum at about 400 nm; whereas the Q band is more characteristic for the nature of the porphyrin, i.e. the substituent at the periphery and the presence or absence of the metal center. Typically, all macrocyclic dyes exhibit rather narrow absorption bands. Thus only partial absorption of the solar spectrum is possible and the solar energy conversion efficiency is expected to be intrinsically low. Compound **5** shows an absorption spectrum similar to $[Ru(bpy)_2(dmbpy)]Cl_2$ [14] with the MLCT band at around 460 nm. The characteristic spectral data are summarized in Table 1.

Strongly colored $TiO_2$ electrodes can be prepared from dyes **1**–**5** if – and only if – membrane modified $TiO_2$ electrodes with the oppositely charged head group are used, as expected from Fig. 1. The photographs of the dye loaded electrodes are presented in Fig. 2b.

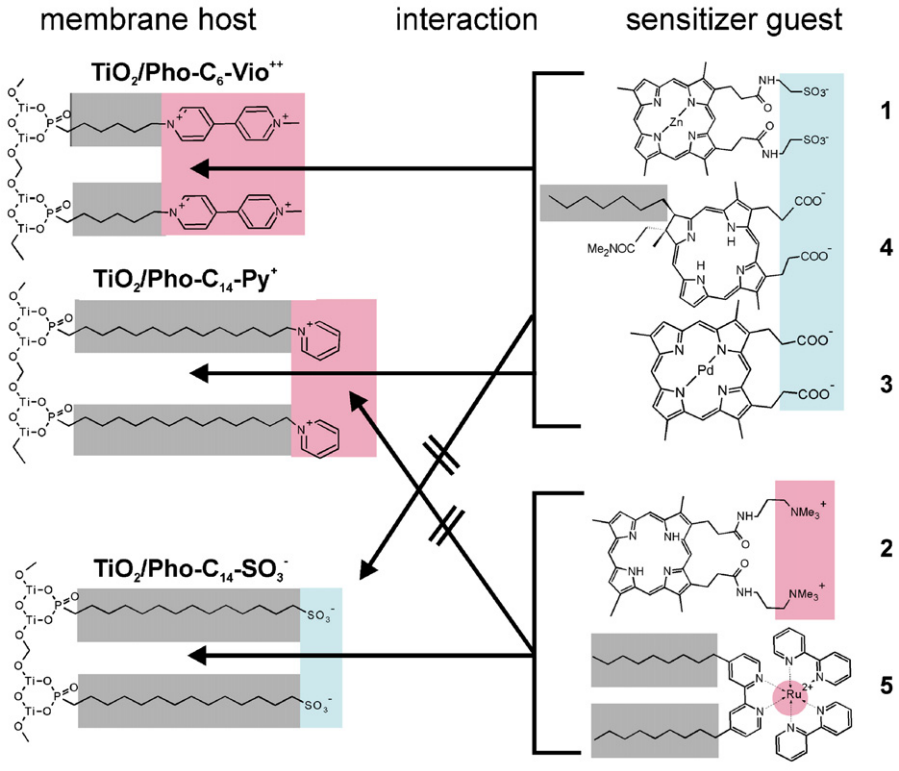


**Fig. 1.** Structure of dyes **1**–**5** for sensitization (right) and membrane molecules coordinated to $TiO_2$ (left) with possible interactions between membrane and dyes (center), color codes: hydrophobic interaction (gray), coulombic interaction (pink (positive) with light blue (negative)). (For interpretation of the references to color in this figure legend, the reader is referred to the web version of the article.)

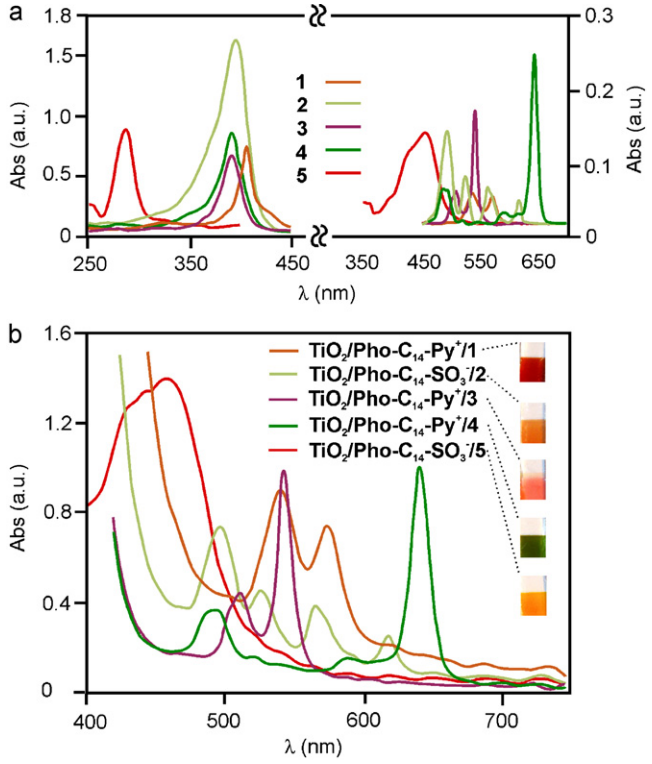


**Fig. 2.** UV–vis absorption spectra of dyes **1**–**5**, (a) in solution (**1**–**4** (THF:MetOH (1:1)), **5** ($H_2O$)); (b) in dry state on $TiO_2$/membrane (only above 400 nm because of $TiO_2$ absorption for λ < 400 nm (blank: unmodified $TiO_2$), and photographs of the modified electrodes.

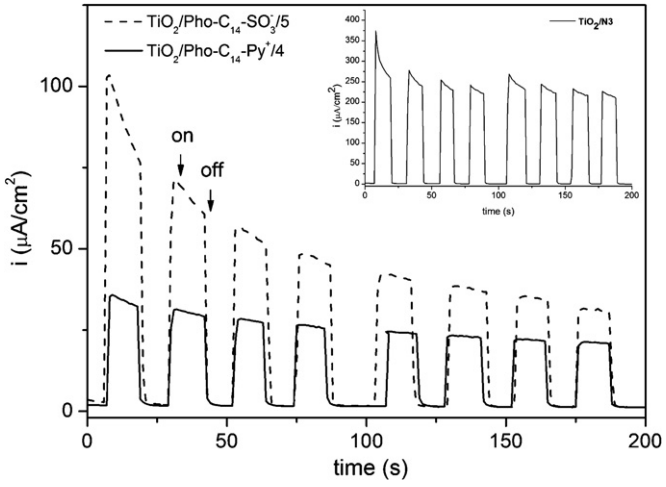


**Fig. 3.** Photocurrent vs. time of $TiO_2$/Pho-$C_{14}$-$Py^+$/4, $TiO_2$/Pho-$C_{14}$-$SO_3^-$/5 and $TiO_2$/N3 (inset) in $H_2O$/0.1 M KI in a 3-electrode system at $E$ = 0.2 V (vs. Ag/AgCl) under chopped white light (16.5 mW/cm$^2$) irradiation.

Coloration persists for days in solution and for months in the dry state. Their spectra exhibit similar features as in solution except for a red shift of the maxima (Fig. 2b and Table 1). This may be due to aggregation of the dyes in the adsorbed state [15] a phenomenon well known for porphyrins even in solution at very low concentration and generally less prominent for the bulkier chlorin [16]. Interestingly, the extent of the red shift is smaller if the membrane is used to hold them as compared to those dyes directly attached to $TiO_2$, indicating that the dye molecules are more diluted when hold by the membrane as compared to direct $TiO_2$ anchoring. This is experimentally confirmed by absorbance measurements yielding the ratio of surface concentrations for direct ($\Gamma_{TiO_2-dye}$) in the range of 0.5. The absolute values of ($\Gamma_{TiO_2-dye}$) for **3** and **4** are in agreement with those of metallo-meso-porphyrins reported earlier [15a] (Table 1 and Fig. 2c). Obviously, the membrane plays a similar role as co-adsorbents which are used to improve the photovoltaic response by suppressing the aggregation of dye molecules on $TiO_2$ [3a,3b,4a,17]. Most importantly, the only way to immobilize dyes **2** and **5** without a typical anchoring group is by using the membrane as a mediator.

On the other hand, in a water-acetontrile (1:1) mixture the membrane confined dyes are not stable, the absorbance of the photoanode, in this case, $TiO_2$/Pho-$C_{14}$-$SO_3^-$/5 decreases by 70% in 2 min (Supporting Information, Fig. 4a). Under such conditions the dye leaves the membrane and the membrane persists. This suggests the need of water as solvent electrolyte for membrane confined dyes.

The values of the surface concentrations of porphyrins or chlorin on a membrane modified electrode are reduced by >50% compared to the directly attached on $TiO_2$ (Table 1).

The chopped white light photocurrent of $TiO_2$/Pho-$C_{14}$-$Py^+$/4 and $TiO_2$/Pho-$C_{14}$-$SO_3^-$/5 under potentiostatic conditions in a 0.1 M KI aqueous electrolyte is presented in Fig. 3. In the inset, the response of the membrane-free standard $TiO_2$-N3 under the same experimental conditions is depicted. The initial photocurrents follow the order i($TiO_2$/N3) ≫ i($TiO_2$/Pho-$C_{14}$-$SO_3^-$/5) ≫ i($TiO_2$/Pho-$C_{14}$-$Py^+$/4), possibly related to (i) a narrower absorption band of **4** and **5** as compared to N3 and/or (ii) a lower electron injection efficiency for the membrane based cases. However, it is yet clear that the membrane does not behave as an insurmountable barrier for electron transfer.

A decay of the photocurrent with illumination time is observed for, $TiO_2$/Pho-$C_{14}$-$Py^+$/4 and $TiO_2$/Pho-$C_{14}$-$SO_3^-$/5 but not for $TiO_2$/N3. It cannot be explained by a loss of the dye into the solution, as no absorbance change of the electrodes is observed after photocurrent measurement. The decrease is more severe for electrodes modified with the phosphonic acids bearing the –$SO_3^-$ head group (Fig. 3, dotted trace) than that bearing the pyridinium group (solid line). One explanation could be that the sulphonate head groups lower the local concentration of iodide, and thus reduce the rate of reduction of the oxidized dye, which may ultimately undergo irreversible chemical reactions. Additionally, there is no influence of the iodide concentration on the photocurrent. As the membrane modification leads to a narrowing and possibly clogging of bottle necks in the mesoporous system, mass transfer limitations of the mediator may also be invoked. Photocurrent decay has been earlier reported for lipid based photoelectrochemical cells [6b,18] possibly because of the increased local concentration of $I_3^-$.

The light chopped current behavior of dyes **5** and **3** as a function of the bias voltage vs. Ag/AgCl on a membrane modified $TiO_2$ electrode is depicted in Fig. 4. It allows to qualitatively judge the photocurrent and the dark current in a single scan. Obviously, the cathodic dark current (related to $I_3^-$ reduction) is more prominent on the membrane with positive head groups than on the membrane with negative head groups, probably because of the increased local concentration of $I_3^-$ on pyridinium. The same trend is observed by cyclic voltammetry on differently modified electrodes, i.e. the absolute value of the cathodic dark current (electrochemical reduction of $I_3^-$) follows the trend $TiO_2$/Pho-$C_{14}$-$Py^+$ > $TiO_2$ < $TiO_2$/Pho-$C_{14}$-$SO_2^-$ ≈ $TiO_2$/$TiCl_4$ (Supporting Information, Fig. 2).

The photo-action spectra of the membrane confined dyes **3** and **5** are shown in Fig. 5. The electrodes yield a maximum current at 545 and 460 nm, respectively, in agreement with their absorption spectra. For comparison the photo-action spectrum of the standard N3 dye directly attached to $TiO_2$ without membrane is presented under the same conditions. As compared to organic solvent/electrolyte systems (Fig. 5b), the APCE of $TiO_2$/N3 in the

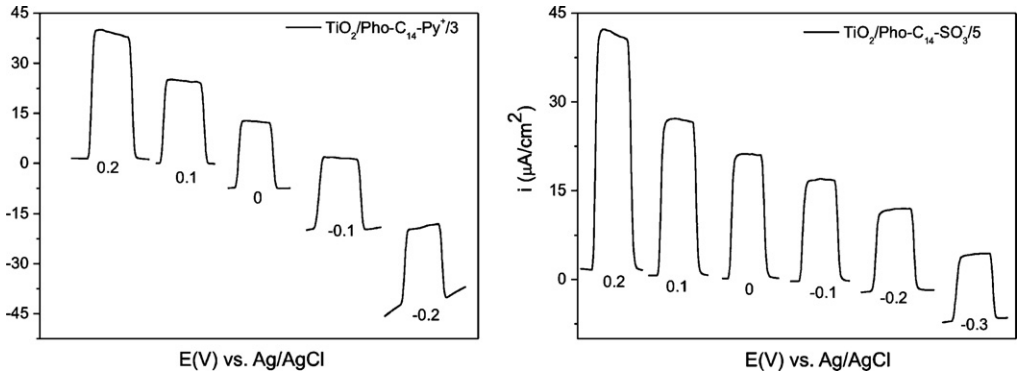


**Fig. 4.** Light chopped photocurrent at different bias potential vs. Ag/AgCl. Experimental condition same as in Fig. 3.

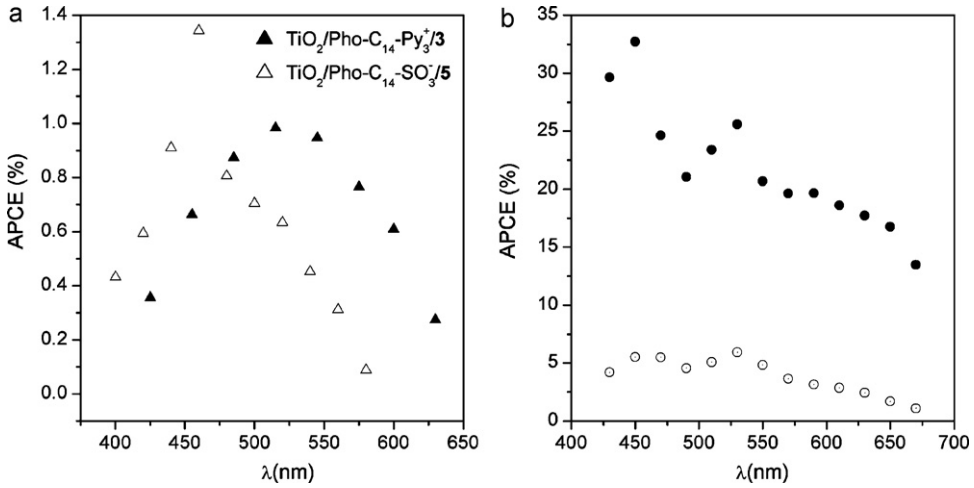


**Fig. 5.** APCE spectra of (a) $TiO_2$/Pho-$C_{14}$-$Py^+$/3 and $TiO_2$/Pho-$C_{14}$-$SO_3^-$/5 and (b) $TiO_2$/N3 in $H_2O/I^-$ electrolyte (open circle) and $TiO_2$/N3 in $CH_3CN/I^-$ electrolyte.

aqueous electrolyte is drastically lowered (no desorption was observed for illumination times in the range of minutes). This is mainly attributed to the loss of photocurrent due to the back electron transfer. This is shown by improved photocurrent after the treatment of $TiCl_4$ (Supporting Information, Fig. 3). Additionally, in aqueous electrolyte the formation of $Ti\text{-}O^-H^+$ will accelerate the back electron transfer with protons acting as surface traps, and water assisted desorption of the dye from the semiconductor surface are possible pathways for photocurrent loss [5a,19]. No discoloration of the films during photocurrent measurements was observed when the aqueous electrolyte was used. Notably, the APCEs of the membrane bound dyes **3** and **5** are lower by a factor of ca. 4 as compared to the $TiO_2$ coordinated N3. This can be interpreted as reduced charge injection efficiency related to the length of the electron transfer path beside. Additionally, most organic dyes exhibit lower efficiencies compared to Ru-based dyes due to accelerated recombination [20]. This is attributed to the ability of these dyes to form complexes with iodine or triiodide which results high local concentration of iodine or quenching of the excited sate [21].

Most interestingly, all the negatively charged macrocyclic dyes in our study show higher currents when coordinated via the pyridinium membrane as compared to the situation when they are directly attached to $TiO_2$ (Fig. 6). This is attributed mainly to the hydrophobic part of the membrane which shields recombination centers and consequently enhances photocurrent [22]. The second reason could be that the pyridinium head groups fulfill a sec-

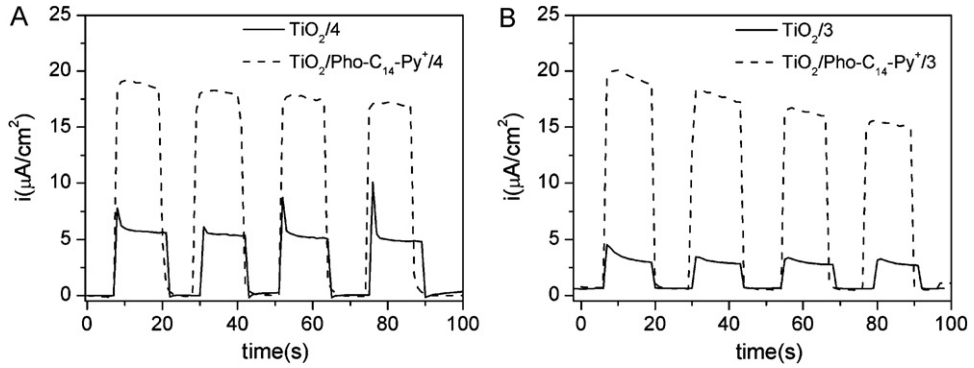


**Fig. 6.** Chopped photocurrent at membrane confined vs. directly $TiO_2$ attached dyes (A) chlorin (**4**) and (B) porphyrin (**3**); experimental condition as in Fig. 3.

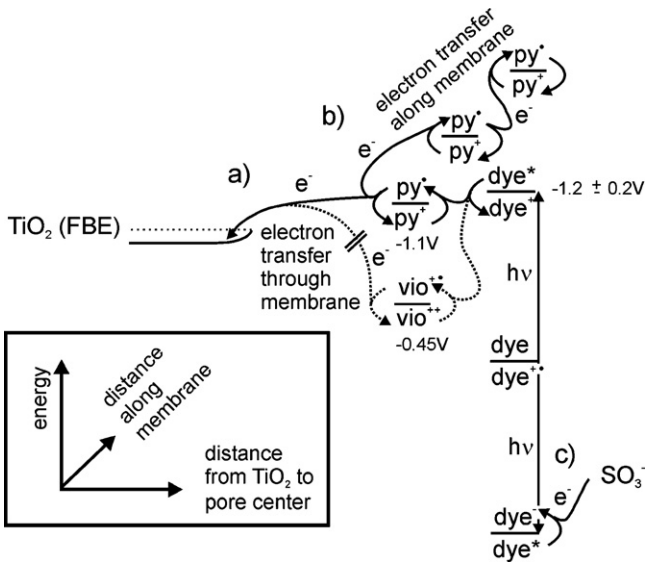


**Fig. 7.** Energetics at the $TiO_2$-membrane-headgroup-sensitizer assembly (a) with pyridinium head groups and oxidative quenching (sensitizer to $py^+$ (**1**, **3** and **4** in Supporting Information)), and (b) with e.t. shuttling between $py^+$/py couples along the membrane followed by electron injection into $TiO_2$, or (c) with (hypothetical) reductive excited state quenching by the membrane sulfonate groups (sulfo to sensitizer). FBE = flat band edge.

ond function besides delivering the positive charge for holding the negatively charged dyes electrostatically. We have evidence, that they assist the electron transfer from the excited state of the dye in to the $TiO_2$ CB. This is supported by the CV of pyridinium modified $TiO_2$ electrodes showing an irreversible wave around −1.1 V (vs. Ag/AgCl) in 0.1 M KCl (Supporting Information) in agreement with literature values [23]. This value is located between the

**Table 2**
Photovoltaic performance of dye sensitized membrane modified $TiO_2$ electrodes.

| Electrode | $J_{SC}$ (μA cm$^{-2}$) | APCE (%) |
|---|---|---|
| $TiO_2$/Pho-$C_{14}$-$SO_3^-$/2 | 22 | 0.5 |
| $TiO_2$/Pho-$C_{14}$-$Py^+$/3 | 36 | 1.0 |
| $TiO_2$/Pho-$C_{14}$-$Py^+$/4 | 15 | 1.5 |
| $TiO_2$/Pho-$C_{14}$-$SO_3^-$/5 | 45 | 1.3 |
| $TiO_2$/N3 | 250 | 5.6 |
| $TiO_2$/N3 in MeCN | 1140 | 33 |

excited state reduction potential of the sensitizers **5**, N3 or **1**–**4** ($E_{dye^*/dye+}$ = −1 V to −1.5 V (Supporting Information)) and the flat band potential of $TiO_2$ (−0.72 V at pH 6) [24].

Furthermore, electrodes modified with a phosphonated viologen $TiO_2$/Pho-$C_6$-$Vio^{2+}$ (Fig. 1) can hold the negatively charged dyes as the $TiO_2$/PhO-$C_{14}$-$Py^+$ membrane does, however, no photocurrent response is observed. This is definitely related to the more positive reduction potential of the bipyridinium cation (−0.5 V), i.e. the viologen acts as a potential sink, whereas pyridinium (−1.1 V) acts as an intermediate injector (Fig. 7).

A semiempirical ZINDO calculation supports this second function of the pyridinium head group, i.e. acting as an intermediate electron acceptor, even on the timescale of electron excitation (see Section 3.1).

In Table 2 the photovoltaic performance of the different dye sensitized membrane modified electrodes using the aqueous $I^-$ electrolyte are presented. The new dyes confined on the membranes show better performance in terms the short circuit current ($J_{SC}$) as compared to the situation when they are directly coordinated to the mesoporous $TiO_2$ (without membrane); **5** being the highest followed by the **3**. On the other hand, dye **1** with two sulfonic acid groups shows the lowest performance with a photocurrent less than 1 μA/cm$^2$. Interestingly, mesoporous $TiO_2$ electrodes sensitized with N3 dye exhibit low APCE even in organic

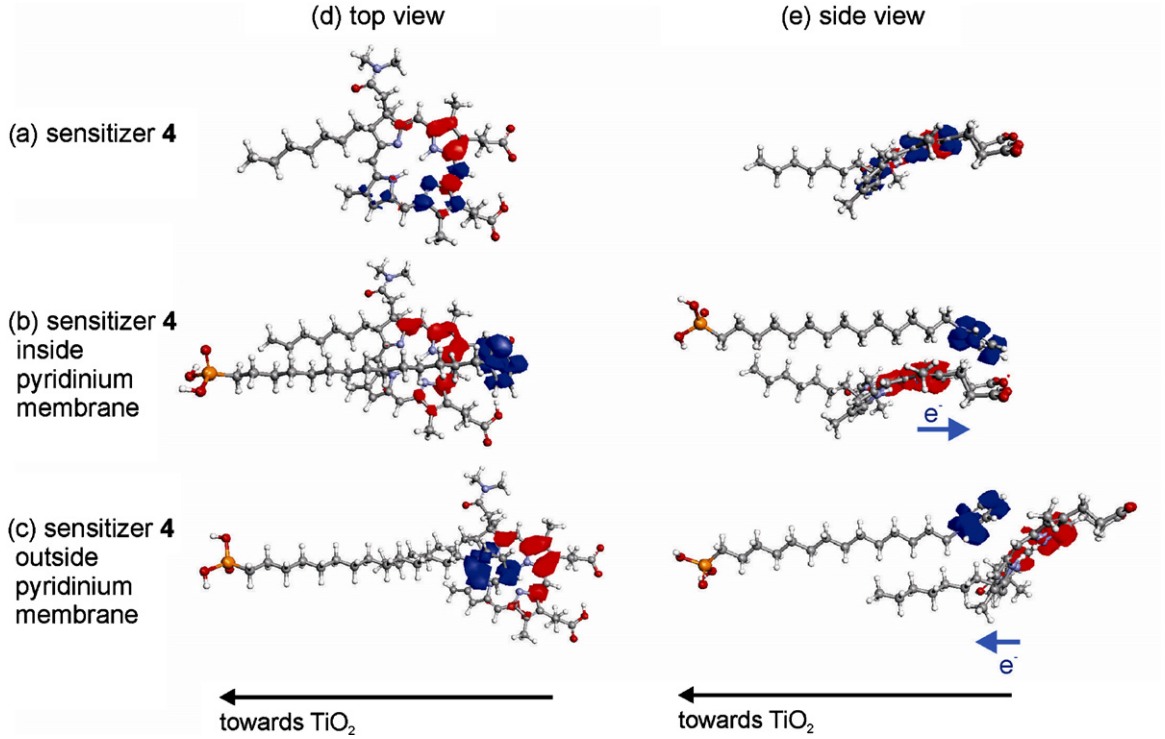


**Fig. 8.** Electron density difference of the first excited minus the ground state (blue: increased electron density, red: decreased electron density, contour value: 0.002) from ZINDO calculations using 10 CI states (singlet excitations) (a) in the isolated sensitizer **4**, (b) and (c) with sensitizer **4** in the presence of a pyridinium membrane molecule, (b) senstizer **4** between pyridinium and $TiO_2$, (c) pyridinium between sensitizer **4** and $TiO_2$; black arrows: towards $TiO_2$, blue arrows: movement of electron density. (For interpretation of the references to color in this figure legend, the reader is referred to the web version of the article.)

electrolyte. This suggests that these electrodes may have had inherently low performance related to the size of the $TiO_2$ particles or morphology of the film. Electrodes treated with $TiCl_4$ shows a 30–40% increase in photocurrent (Fig. 3 of Supporting Information).

### 3.1. The influence of the membrane pyridinium on photo-induced charge separation: ZINDO calculation

Besides electrostatically binding the sensitizer to the outer membrane surface, the pyridinium and sulfonate head groups may also assist or tune the photo-induced charge separation. This is demonstrated by semiempirical ZINDO/S calculations.

Such calculations on the sensitizers **1**, **2**, **3** (with Pd replaced by Zn because of missing parameters), **4** and **5** (Ru replaced by Fe) revealed the following:

(i) The excited states of the isolated sensitizers **1**–**5** calculated in the absence of a membrane compound show all intra-molecular charge dislocation upon photoexcitation, i.e. photoexcited charge separation occurs only within the porphyrin. This qualitative analysis is based on the corresponding electron density difference maps of the first excited state with respect to the ground state (Fig. 8a).
(ii) The excited states of sensitizers **1**, **3** and **4** calculated in proximity (ca. 0.2–1 nm) of the pyridinium terminated alkyl phosphonate show efficient population of the pyridinium $\pi^*$ system with electron density stemming from the dye upon photoexcitation in agreement with electrochemical and fluorescence measurements. Fig. 8 shows the distribution of the excited state electron density dislocation for compound **4** in the presence of a alkyl pyridinium ion.
(iii) The relative orientation of the dye to the pyridinium (or to a smaller extent to the sulphonate) is important for the direction of the charge shift either towards or away from $TiO_2$, however, the relative position of dye and pyridinium is not known.
(iv) Beside direct charge injection from the first photo-generated pyridine radical, one can envisage an electron hoping process involving many pyridinium head groups, which drives the electron away from the oxidized sensitizers towards sites with facilitated $TiO_2$ electron injection kinetics (Fig. 7). Such a lateral electron hoping mechanisms on membrane modified $TiO_2$ has been described earlier [13].
(v) The sulfonated membranes can act as a donor (in contrast to pyridinium) in the photoexcited state (Fig. 7).

## 4. Conclusion

Nature uses double membranes which only can exist in an aqueous system and proteins as a scaffold for the right positioning of sensitizer and redox mediators in space to achieve photo-induced charge separation. In a DSSC based on a dye sensitized $TiO_2$ electrode it is a dogma to use organic solvents and no water, because with all water based electrolytes reduced efficiencies are observed (the rationale behind this is still not clear). Furthermore, the dyes are directly coordinated onto the $TiO_2$ surface.

We have introduced a membrane onto the inner wall of mesoporous $TiO_2$ using different alkyl phosphonates with charged head groups. Obviously, this membrane persists only in an aqueous system. The dyes are coordinated to the charged surface of the outer membrane by a combination of hydrophobic and electrostatic interactions – similarly as observed in nature.

Principally this architecture allows for new architectural complexity on the molecular level. The results show:

(i) Electron transfer can occur through the membrane into $TiO_2$.
(ii) Some dyes show better injection efficiencies when placed onto the membrane as compared to the case when they are directly coordinated to the $TiO_2$.
(iii) The pyridinium unit of the membrane can act as an intermediate electron acceptor, as supported by experimental and theoretical results.

It is expected that the performance can be enhanced by introducing a $TiCl_4$-blocking layer, by optimizing the $TiO_2$ layer thickness. Optimization of these parameters and investigation of charge injection mechanism is under way.

## Acknowledgements

We are very grateful to Dr. Nick Vlachopoulos for fruitful discussions. D.H.T. thanks the federal state of Lower Saxony (Lichtenberg-Stipendium), and M.K. thanks the graduate college 612 funded by the DFG for financial support.

## Appendix A. Supplementary data

Supplementary data associated with this article can be found, in the online version, at doi:10.1016/j.jphotochem.2010.09.003.

## References

[1] A. Hagfeldt, M. Graetzel, Chem. Rev. (Washington, D.C.) 95 (1995) 49.
[2] M. Gratzel, J. Photochem. Photobiol. C 4 (2003) 145.
[3] (a) P. Wang, S.M. Zakeeruddin, R. Humphry-Baker, J.E. Moser, M. Gratzel, Adv. Mater. 15 (2003) 2101;
(b) P. Wang, C. Klein, R. Humphry-Baker, S.M. Zakeeruddin, M. Gratzel, Appl. Phys. Lett. 86 (2005) 3;
(c) J.E. Kroeze, N. Hirata, S. Koops, M.K. Nazeeruddin, L. Schmidt-Mende, M. Graetzel, J.R. Durrant, J. Am. Chem. Soc. 128 (2006) 16376.
[4] (a) X. Li, H. Lin, S.M. Zakeeruddin, M. Gratzel, J.B. Li, Chem. Lett. 38 (2009) 322;
(b) M.K. Wang, C. Gratzel, S.J. Moon, R. Humphry-Baker, N. Rossier-Iten, S.M. Zakeeruddin, M. Gratzel, Adv. Funct. Mater. 19 (2009) 2163;
(c) Z.P. Zhang, S.M. Zakeeruddin, B.C. O'Regan, R. Humphry-Baker, M. Gratzel, J. Phys. Chem. B 109 (2005) 21818.
[5] (a) P. Liska, N. Vlachopoulos, M.K. Nazeeruddin, P. Comte, M. Gratzel, J. Am. Chem. Soc. 110 (1988) 3686;
(b) T.N. Murakami, H. Saito, S. Uegusa, N. Kawashima, T. Miyasaka, Chem. Lett. 32 (2003) 1154.
[6] (a) W.H. Lai, Y.H. Su, L.G. Teoh, M.H. Hon, J. Photochem. Photobiol. A 195 (2008) 307;
(b) K. Jiang, H. Xie, W. Zhan, Langmuir 25 (2009) 11129;
(c) K. Wongcharee, V. Meeyoo, S. Chavadej, Sol. Energy Mater. Sol. Cells 91 (2007) 566.
[7] Y.H. Su, W.H. Lai, L.G. Teoh, M.H. Hon, J.L. Huang, Appl. Phys. A 88 (2007) 173.
[8] M.R. Wasielewski, Acc. Chem. Res. 42 (2009) 1910.
[9] (a) J.B. Asbury, E. Hao, Y. Wang, H.N. Ghosh, T. Lian, J. Phys. Chem. B 105 (2001) 4545;
(b) M. Nilsing, P. Persson, S. Lunell, L. Ojamaee, J. Phys. Chem. C 111 (2007) 12116;
(c) M. Gratzel, Pure Appl. Chem. 73 (2001) 459.
[10] (a) D. Taffa, M. Kathiresan, L. Walder, Langmuir 25 (2009) 5371;
(b) D.H. Taffa, M. Kathiresan, L. Walder, B. Seelandt, M. Wark, Phys. Chem. Chem. Phys. 12 (2010) 1473.
[11] K.M. Smith, Porphyrins and Metalloporphyrins, 1975.
[12] (a) F.P. Montforts, A. Meier, G. Haake, F. Hoeper, Tetrahedron Lett. 32 (1991) 3481;
(b) D. Kusch, A. Meier, F.P. Montforts, Liebigs Ann. (1995) 1027;
(c) F.-P. Montforts, M. Glasenapp-Breiling, Prog. Heterocycl. Chem. 10 (1998) 1.
[13] Q. Wang, S.M. Zakeeruddin, M.K. Nazeeruddin, R. Humphry-Baker, M. Graetzel, J. Am. Chem. Soc. 128 (2006) 4446.
[14] D. Hesek, Y. Inoue, S.R.L. Everitt, H. Ishida, M. Kunieda, M.G.B. Drew, Inorg. Chem. 39 (2000) 308.
[15] (a) A. Kay, M. Gratzel, J. Phys. Chem. 97 (1993) 6272;
(b) Y. Fujii, Y. Hasegawa, S. Yanagida, Y. Wada, Chem. Commun. (2005) 3065.
[16] K. Kalyanasundaram, M. Gratzel, Coord. Chem. Rev. 177 (1998) 347.
[17] P. Wang, S.M. Zakeeruddin, P. Comte, R. Charvet, R. Humphry-Baker, M. Gratzel, J. Phys. Chem. B 107 (2003) 14336.
[18] (a) K.C. Hwang, D. Mauzerall, Nature 361 (1993) 138;
(b) S.Y. Huang, G. Schlichthorl, A.J. Nozik, M. Gratzel, A.J. Frank, J. Phys. Chem. B 101 (1997) 2576;
(c) J.J. Nelson, T.J. Amick, C.M. Elliott, J. Phys. Chem. C 112 (2008) 18255;

(d) M. Wang, P. Chen, R. Humphry-Baker, S.M. Zakeeruddin, M. Gratzel, Chemphyschem 10 (2009) 290.
[19] H. Saito, S. Uegusa, T.N. Murakami, N. Kawashima, T. Miyasaka, Electrochemistry 72 (2004) 310.
[20] B.C. O'Regan, I. Lopez-Duarte, M.V. Martinez-Diaz, A. Forneli, J. Albero, A. Morandeira, E. Palomares, T. Torres, J.R. Durrant, J. Am. Chem. Soc. 130 (2008) 2906.
[21] K.E. Splan, A.M. Massari, J.T. Hupp, J. Phys. Chem. B 108 (2004) 4111.
[22] (a) A.J. Frank, N. Kopidakis, J. van de Lagemaat, Coord. Chem. Rev. 248 (2004) 1165;
(b) N. Kopidakis, N.R. Neale, A.J. Frank, J. Phys. Chem. B 110 (2006) 12485.
[23] (a) J. Grimshaw, S. Moore, N. Thompson, J. Trochagrimshaw, Chem. Commun. (1983) 783;
(b) J. Volke, L. Dunsch, V. Volkeova, A. Petr, J. Urban, Electrochim. Acta 42 (1997) 1771;
(c) A. Brisach-Wittmeyer, S. Lobstein, M. Gross, A. Giraudeau, J. Electroanal. Chem. 576 (2005) 129.
[24] G. Rothenberger, D. Fitzmaurice, M. Gratzel, J. Phys. Chem. 96 (1992) 5983.